

Hysteretic properties of a magnetic particle with strong surface anisotropy

M Dimian and H Kachkachi*

*Laboratoire de Magnétisme et d'Optique, Université de Versailles St. Quentin,
45 av. des Etats-Unis, 78035 Versailles, France*

February 7, 2020

We study the influence of surface anisotropy on the zero-temperature hysteretic properties of a small single-domain magnetic particle, and give an estimation of the anisotropy constant for which deviations from the Stoner-Wohlfarth model are observed due to non-uniform reversal of the particle's magnetisation. For this purpose, we consider a spherical particle with simple cubic crystalline structure, a uniaxial anisotropy for core spins and radial anisotropy on the surface. The hysteresis loop is obtained by solving the local (coupled) Landau-Lifschitz equations for classical spin vectors. We find that when the surface anisotropy constant is at least of the order of the exchange coupling, large deviations are observed with respect to the Stoner-Wohlfarth model in the hysteresis loop and thereby the limit-of-metastability curve, since in this case the magnetisation reverses its direction in a non-uniform manner via a progressive switching of spin clusters. In this case the critical field, as a function of the particle's size, behaves as observed in experiments.

PACS number(s): 75.50.Tt - 75.30.Pd - 75.10.Hk

I. INTRODUCTION

Surface effects have a strong bearing on the properties of small magnetic systems, and entail large deviations from the bulk behaviour. It was shown in [1] (and references therein) that the magnetic disorder on the surface caused by surface anisotropy is long range, which implies that even the spins in the core of a very small magnetic particle (2 nm) render a magnetisation that deviates from the bulk value. It will be useful to understand surface effects in magnetic materials in order to control their properties which are relevant for technological applications. One such property is the coercive field as it gives indications on the relaxation time of the magnetisation and thereby the stability of the information stored on magnetic media.

Surface effects are due to the breaking of crystal-field symmetry, and this is a local effect. So, in order to study such effects one has to resort to microscopic theories, unlike the macroscopic Stoner-Wohlfarth (SW) model [2], which are capable of distinguishing between different atomic environments and taking account of physical parameters such as bulk and surface anisotropy, exchange and dipole-dipole interactions. Unfortunately, this leads to difficult many-body problems which can only be dealt with using numerical approaches.

In this work, we deal with the effect of strong surface anisotropy on the hysteretic properties (hysteresis loop and limit-of-metastability curve, the so-called SW astroid), of a single-domain spherical particle (with free surfaces), a simple cubic (sc) crystalline structure, a uniaxial anisotropy in the core, and radial single-site anisotropy for spins on the boundary. The hysteresis loop and thereby the critical field are computed by solving, at zero temperature, the local Landau-Lifshitz equation derived from the classical anisotropic Dirac-Heisenberg model in field, subjected to a local condition (see below) accounting for the minimisation of energy with respect to local rotations of each spin in the particle. In Ref. [3] the same method was used for studying the hysteretic properties of models of nanoparticles, where the anisotropy was either random in the whole particle or taken only on the surface, and the analysis was restricted to the hysteresis loop.

In our work, we use an improved version of the method mentioned above including a global-rotation condition on the resultant magnetic moment of the particle in addition to the local condition (see [4]). We compute the hysteresis loop and infer from it the limit-of-metastability curve (SW astroid), and compare with the SW model especially when the surface anisotropy constant assumes large values, e.g. $K_s \gtrsim J$. This study has allowed us to investigate the limit of validity of the SW model for very small magnetic particles where surface anisotropy plays a determinant role, and whose magnetisation no longer switches in a coherent manner.

Our method, based on the numerical solution of the Landau-Lifshitz equation at zero temperature, is checked against the SW semi-analytical results in two limiting cases of the exchange coupling with different distributions of anisotropy axes. We first consider a single-domain particle with a macroscopic magnetic moment resulting from very strong exchange interaction. This is equivalent to the SW one-spin problem with uniaxial anisotropy. A second test considers the case of a square particle of non-interacting spins all with randomly distributed easy axes. This model

mimics an assembly of single-domain nanoparticles with a random distribution of their easy axes embedded in a 2d non-magnetic matrix.

The plan of this work is as follows: we first define our model (Hamiltonian and physical parameters), present the method used for computing the hysteresis loop, and test it against the semi-analytical results of SW model. Then, we discuss our results for a spherical particle in terms of exchange coupling, particle's size, and surface anisotropy by varying, in turn, one of them while keeping the other two fixed. It is worth mentioning though that in reality, only surface anisotropy can be considered as a free parameter as there are so far no definite experimental estimation thereof.

II. MODEL HAMILTONIAN

We consider the following classical anisotropic Dirac-Heisenberg model

$$\mathcal{H} = -J \sum_{\langle i,j \rangle} \mathbf{S}_i \cdot \mathbf{S}_j - (g\mu_B) \mathbf{H} \cdot \sum_{i=1}^{\mathcal{N}} \mathbf{S}_i + H_{an}, \quad (1)$$

where \mathbf{S}_i is the unit spin vector on site i , \mathbf{H} is the uniform magnetic field applied in a direction ψ with respect to the reference z axis, \mathcal{N} is the total number of spins (core and surface); J is the strength of the nearest-neighbour exchange interaction, which will be taken in our calculations the same everywhere inside the particle; H_{an} is the uniaxial anisotropy energy

$$H_{an} = - \sum_i K_i (\mathbf{S}_i \cdot \mathbf{e}_i)^2, \quad (2)$$

with easy axis \mathbf{e}_i and constant $K_i > 0$. This anisotropy term contains either of the two contributions stemming from the core and surface, and depends on the model used. For instance, for the 2d model (which serves as a test of our calculations by comparison with the SW model) all spins (core and surface) have the same anisotropy constant but randomly distributed axes. In the case of a spherical particle, all core spins are attributed the same constant K_c and all surface spins are attributed the constant K_s . Moreover, core spins will have an easy axis along the z axis, whereas a surface spin is assumed to have its anisotropy axis along the radial direction.

III. METHOD OF CALCULATION OF THE HYSTERESIS LOOP

Different models of a nanoparticle are studied. In each case, we simulate the lattice with sc crystal structure, and then assign to each site a length-fixed three-component spin vector. For the calculation of the hysteresis loop we start with a magnetic configuration where all spins are pointing in the same direction $-z$, which corresponds to the saturation state. The hysteresis loop is due the existence of metastable states in the system. Starting from the initial configuration and applied field, the integration of the Landau-Lifshitz equation (see below) tends towards a new configuration that is an energy minimum.

Let us now establish the Landau-Lifshitz equations for the magnetic moments. We choose K_c as the energy scale and normalise the other physical constants accordingly, i.e.,

$$t \rightarrow \frac{2K_c}{\hbar} \times t, \quad \mathbf{h} \equiv \frac{(g\mu_B)}{2K_c} \times \mathbf{H}. \quad (3)$$

Then, the Landau-Lifshitz (LL) equation for a spin \mathbf{S}_i at site i , reads

$$\frac{d\mathbf{S}_i}{dt} = -\mathbf{S}_i \times \mathbf{h}_i^{eff} - \alpha \mathbf{S}_i \times (\mathbf{S}_i \times \mathbf{h}_i^{eff}) \quad (4)$$

where $\alpha (\sim 1)$ is the damping parameter and \mathbf{h}_i^{eff} is the effective field acting on the spin \mathbf{S}_i and is given by

$$\mathbf{h}_i^{eff} = \mathbf{h} + \frac{J}{2K_c} \sum_{j=1}^{z_i} \mathbf{S}_j + \mathbf{h}_i^{an} \quad (5)$$

where $\mathbf{h}_i^{an} \equiv -(\partial H_{an}/\partial \mathbf{S}_i)/2K_c$, with H_{an} given in Eq. 2, z_i is the coordination number of site i . In the sequel, we will use the reduced parameters, $j \equiv J/K_c$, $k_s \equiv K_s/K_c$. Therefore, for each site i we arrive at three coupled equations

(for S_i^x, S_i^y, S_i^z), and because of the second term in (5) we actually obtain a system of $3\mathcal{N}$ (local) coupled equations. We emphasise that it is more convenient to use spherical coordinates (for each spin) instead of the Cartesian ones. Indeed, owing to the fact that the spins are of constant length, this reduces the number of individual (for each spin) equations to two instead of three,

$$\begin{aligned}\dot{\theta}_i &= (h_\varphi^{eff} + \alpha h_\theta^{eff})_i \\ \dot{\varphi}_i &= \left(-h_\theta^{eff} + \alpha h_\varphi^{eff}\right)_i / \sin \theta_i,\end{aligned}\tag{6}$$

where $h_\theta^{eff} \equiv -\partial\mathcal{H}/\partial\theta$, $h_\varphi^{eff} \equiv -\partial\mathcal{H}/\partial\varphi$, are the polar components of the effective field. For the one-spin problem, these are obtained by direct differentiation for the energy written in spherical coordinates, whereas for a particle it is not possible to obtain a tractable analytical expression of the energy in spherical coordinates, so h_θ^{eff} and h_φ^{eff} are written in terms of the time derivatives of the Cartesian components of \mathbf{h}_i^{eff} in (5). Using Eq. (6) instead of (4) allows for a gain of computer time, but this method encounters stability problems specific to the spherical coordinates, because of the factor $1/\sin\theta$ in (6), which diverges as $\theta \rightarrow 0, \pi$, and hence a special care is required when numerically handling these equations.

After having constructed the magnetic structure (lattice and spin vectors on it), we apply a magnetic field \mathbf{H} at some angle ψ with respect to the reference z axis, with values chosen in a regular mesh. Then we calculate the local effective field for all spins and thereby the right-hand sides of the LL equations (6) and proceed with the time integration. As this is done, the total energy in Eq.(1) smoothly decreases, and some criterion must be used for stopping the integration for the given value of the applied field and moving to the next value. In our calculations we proceed to the next field value when

$$\frac{1}{N} \sum_{i=1}^N \left| \frac{d\mathbf{S}_i}{dt} \right| < \varepsilon,\tag{7}$$

which implies that the system is close to a stationary state, ε being a small parameter of the order of $10^{-5} - 10^{-7}$. However, it was shown in [4], that this local condition, which accounts for the minimisation of energy with respect to local rotations (or small deviations) of each spin, should be supplemented by a global condition on the resultant magnetic moment so as to account for the global rotation of the particle's magnetic moment. Obviously, for a single spin these two conditions boil down to one and the same condition (7).

Next, the stationary state thus obtained is used as the initial state for the next value of the field. Iteration of this process over a sequence of applied fields, of given magnitude and direction ψ , renders the hysteresis loop. For each pair of these angles we determine the critical or switching field (see discussion below). The whole procedure finally renders the critical or switching field as a function of the angles ψ , which in the case of critical field is the SW astroid.

As a test of this method, we considered a particle with $\mathcal{N} = 3^3$, a sc structure, uniaxial anisotropy, and strong exchange interaction between spins inside the particle, and computed the hysteresis loop for different values of the angle ψ between the applied field and the easy axis. The results are shown in Fig. 1 (left). Next, we present in Fig. 1 (right) the SW astroid, which separates the region with two minima of energy from that with only one minimum. We see that the SW results are faithfully reproduced by our calculations. We have also computed the hysteresis loop of a square particle of non-interacting spins ($J = 0$) all with randomly distributed easy axes. This is equivalent to an assembly of mono-dispersed single-domain non-interacting particles with randomly distributed easy axes in two dimensions. As expected, we find that the remanent magnetisation is equal to $1/2$.

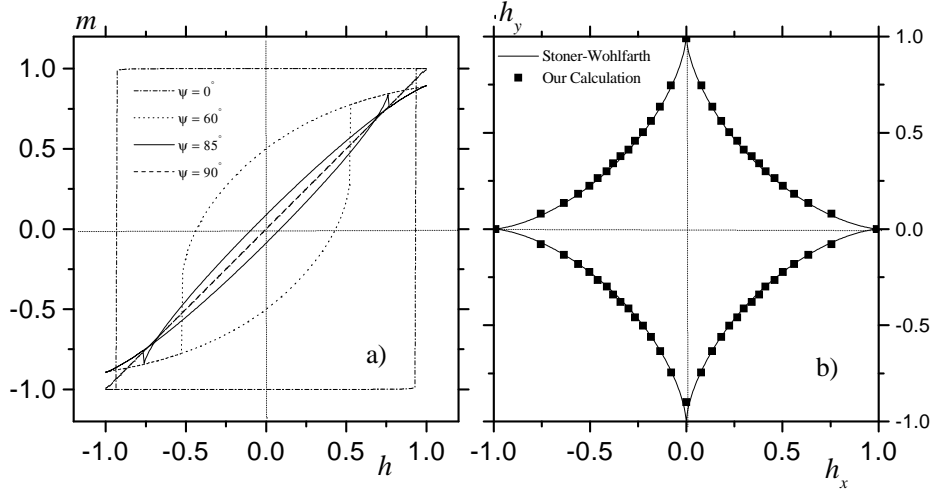


FIG. 1. Left: (numerical) hysteresis loops for different values of ψ increasing inwards: $\psi = 0^\circ, 60^\circ, 85^\circ, 90^\circ$, for a 3^3 particle with uniaxial anisotropy. Right: (numerical in squares and analytical in full line) SW astroid for the same particle; $j = 10$. For the sake of clarity the SW analytical hysteresis loops have been omitted.

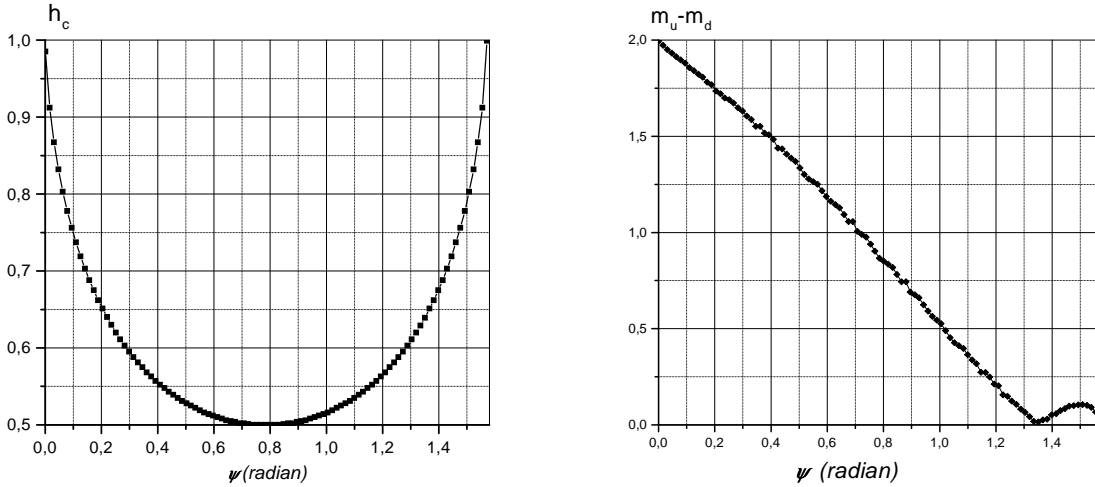


FIG. 2. One-spin problem. Left: critical field as function of ψ . Right: height of magnetisation jump as function of ψ .

For later reference, we plot in Figs. 2 the critical field h_c and the height of the magnetisation jump (i.e. $m_u - m_d$), as functions of angle ψ between the direction of the field and core easy axis. Obviously, $h_c(\psi)$ in Fig. 2 (left) is a well known result of the Stoner-Wohlfarth model. On the other hand, we note that the height of magnetisation jump has an almost linear dependence on ψ , except for the final portion $76^\circ < \psi < 90^\circ$, which corresponds to cycles with crossing branches as exhibited by the hysteresis for $\psi = 85^\circ$ in Fig. 1 (left), see [5] for discussion of this issue.

IV. SPHERICAL PARTICLES: RESULTS AND DISCUSSION

Here we consider a single-domain spherical particle of simple cubic (sc) structure with uniaxial anisotropy in the core and anisotropy constant K_c , and radial anisotropy on the surface with constant K_s . Our main goal here is to investigate the influence of surface anisotropy, both in direction and strength, on the hysteresis loop and SW astroid. However, we will also study the effect of exchange coupling and particle's size.

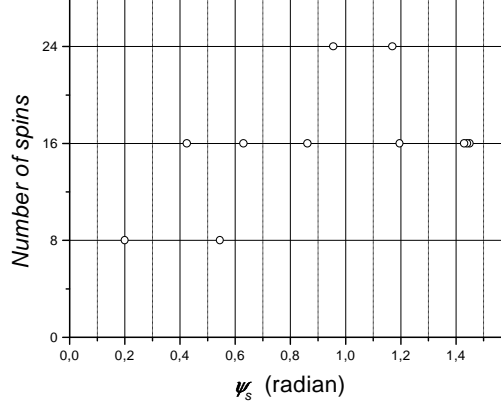


FIG. 3. Distribution of surface anisotropy axes versus the azimuthal angle ψ_s for a spherical particle with $N = 10$ ($\mathcal{N} = 360$: 176 surface spins and 184 core spins).

Again for later reference, we plot in Fig. 3 the distribution of surface anisotropy axes of the spherical particle as a function of the azimuthal angle ψ_s between a surface spin easy axis and applied field.

A. Effect of the exchange coupling j

Now we study the effect of exchange coupling on the hysteresis loop of a spherical particle containing $\mathcal{N} = 360$ spins (176 surface spins and 184 core spins). We first consider the case in which the anisotropy constants in the core and on the surface are equal, i.e. $k_s = 1.0$, and the magnetic field applied along the easy axis of the core spins, since we would like to investigate the influence of radial direction for surface anisotropy.

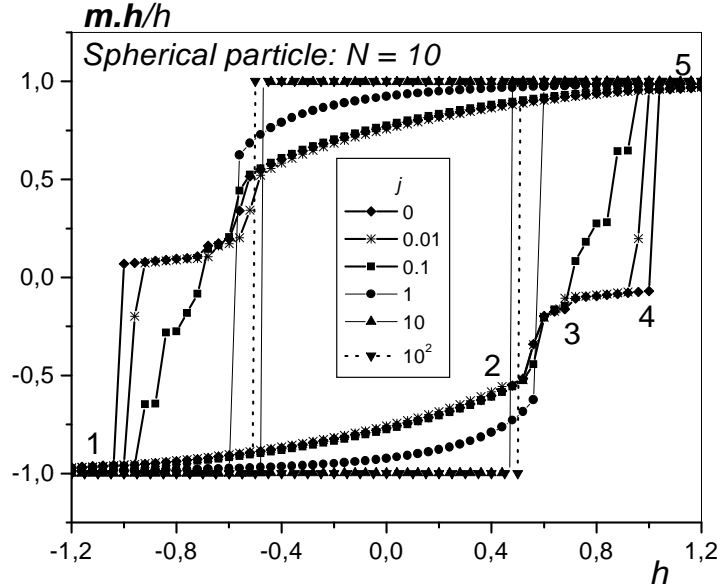


FIG. 4. Hysteresis loop for $\psi = 0$, $k_s = 1$ and different values of j . $\mathcal{N} = 360$.

For $j \ll 1$, i.e. $j = 0, 0.01$, we can see along portion 1-2 in Fig. 4 a progressive decrease (in absolute value) of the magnetisation, which is due to the alignment of surface spins, since as the field direction is along the core easy axis the core spins have a rectangular cycle and the jump is at $h = 1.0$. Next, along portion 2-3 we can see two jumps. Indeed, according to the distribution of surface easy axes in Fig. 3, and the critical field as a function of ψ in Fig. 2 (left), those surface spins with ψ_s between 0.6 and 1.0 are responsible for the first jump, and those with ψ_s between 0.4 and 0.6 or 1.0 and 1.2 are responsible for the second jump. Next, along portion 3-4 we have successive small jumps and thereby a slight decrease of the magnetisation. The origin of these small jumps resides in two contributions. One

contribution comes from those surface spins whose easy axis makes an angle around 0.2 with the field. Even though the corresponding height of jump is large (see Fig. 2, right), their number is rather small (see Fig. 3) thus rendering a small contribution to the magnetisation. The other contribution is due to surface spins with an angle $\psi_s \simeq 1.4$, which yield a small contribution owing to the fact that the height of the corresponding jump is very small (see Fig. 2, $\psi_s > 1.2$), even though their number is relatively large. On the last portion of the lower branch of the hysteresis in Fig. 4, we see another big jump, which is due to the switching of core spins at the field $h_c = 1.0$. At last, there is a slow increase of magnetisation due to a final adjustment of surface spins along the field direction. In the present case, the surface fully switches before the core (see Fig. 5).

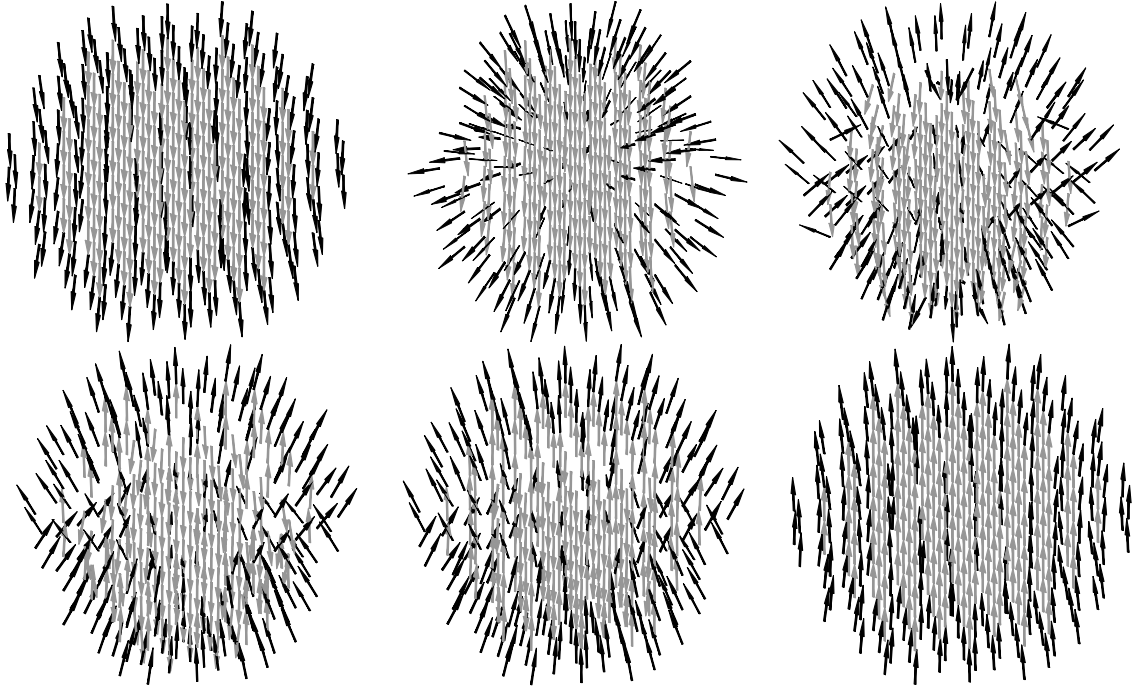


FIG. 5. Magnetic structure for $j = 0.1, k_s = 1$ for the field values $h = -4.0, 0, 0.64, 0.8, 0.88, 4$ which correspond to the saturation states and different switching fields shown in Fig. 4. These field values correspond to the pictures when starting from the upper array and moving right, down left, and then right. Obviously, grey arrows represent core spins and black arrows represent surface spins.

For $j = 0.1$, we see that the surface behaviour remains almost the same as in the previous cases, whereas the core spins now switch cluster-wise as can be seen in the 4th picture of Fig. 5. Indeed, regarding the exchange field as a small perturbation of the applied magnetic field, it is clear that the core spins located near the surface are subject to an effective field whose direction is slightly deviated from their easy axis, i.e. the corresponding angle ψ is slightly different from zero. Now, in Fig. 2 (left) we can see that this little deviation in ψ produces an important change in the switching field. On the contrary, we find that this effect is almost absent in what concerns the jumping field of surface spins, as can be seen along portion 2-3 in Fig. 4 upon comparing the loops for $j = 0, 0.01$ and $j = 0.1$. Indeed, the surface spins responsible for these jumps have their easy axes at an angle $0.6 < \psi_s < 1.0$, and hence the change in the corresponding critical field is very small (see Fig. 2 left). In Fig. 4 we can also see that for $j = 0.1$, i.e. when the exchange energy becomes comparable with anisotropy and Zeeman energy, there are more jumps that can be attributed to the switching of different spherical shells of spins starting from surface down to the centre. This situation is sketched in Fig. 5. For example, for $h = 0$ one can see that the exchange has a little influence on surface spins, as they are directed almost along their easy axes; for $h = 0.64$ the surface spins show the same behaviour as in the absence of exchange, but part of core spins, located near the surface, are deviated from their easy axes. At the field $h = 0.8$ all these core spins have already switched.

For $j = 1 \sim k_s$, even that there is only one jump, the hysteresis loop is not rectangular owing to the fact that the spins rotate in a non-coherent way, as can be seen in Fig. 6. This is due to a compromise between anisotropy and exchange energies, see for example the picture for $h = 0$. Moreover, even a small number of neighbours lying in the core produces a large effect via exchange on the behaviour of a surface spin.

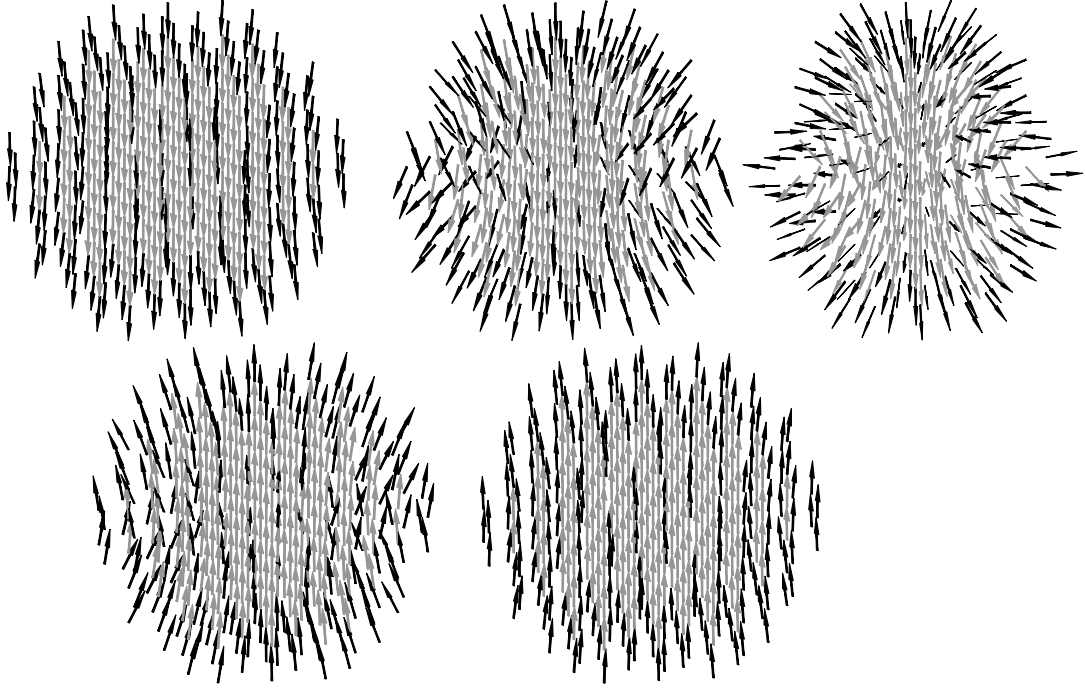


FIG. 6. Magnetic structure for $j = 1, k_s = 1$ for the field values $h = -4.0, 0, 0.56, 0.6, 4$ which correspond to the saturation states and different switching fields shown in Fig. 4. As in Fig. 5, grey arrows represent core spins and black arrows represent surface spins.

For much larger values of j the spins are tightly coupled and move together, and the corresponding (numerically obtained) critical field h_c coincides with the analytical expression obtained in the limit $J \rightarrow \infty$, i.e. $h_c = N_c/\mathcal{N}$, where N_c is the number of core spins. This expression for h_c has been obtained by summing over the direction of surface easy axes which results in a constant surface energy contribution proportional to k_s . Hence, due to spherical symmetry, the surface anisotropy constant does not enter the final expression of h_c .

Now we consider the case of larger values of k_s , e.g. $k_s = 10$, so as to investigate the influence of surface anisotropy both in direction and strength. The results are presented in Fig. 7 (left).

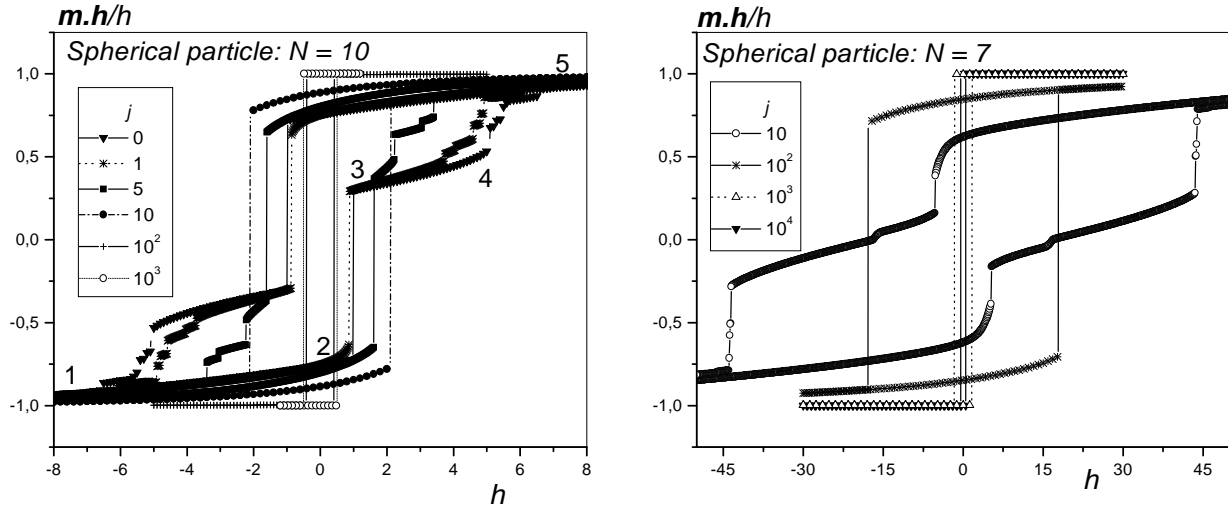


FIG. 7. Left: Hysteresis loops for $\psi = 0, k_s = 10$ and different values of j . $\mathcal{N} = 360$. Right: Hysteresis loops for $\psi = 0, k_s = 10^2$ and different values of j . $\mathcal{N} = 123$.

Here, a notable difference with respect to the previous case, $k_s = 1$, is the fact that the core now switches before the surface and at higher fields. Moreover, there appear more jumps which may be attributed to the switching of

various clusters of surface spins. Both cases show that as the ratio j/k_s decreases, the magnetisation requires higher fields to saturate. This is further illustrated by Fig. 7 (right) where $k_s = 10^2 = j$ for a smaller particle.

Let us now summarise the ongoing discussion. We observe that considering a radial distribution for surface anisotropy, leads, even in the case of very strong exchange, to an important quantitative deviation from the classical SW model. In particular, the critical field in our model is given by

$$H_c^r = \frac{N_c}{N} H_c^u, \quad (8)$$

where H_c^r is the critical field for a spherical particle with radial anisotropy on the surface and uniaxial in the core, H_c^u is the critical field for a spherical particle with uniaxial anisotropy for all spins. Therefore, when j and k_s are comparable, the compromise between exchange coupling, favouring a full alignment of the spins along each other, and surface anisotropy, which favours the alignment of spins along their radial easy axes, produces large deviations from the SW model. More precisely, the shape of the hysteresis loop is no longer rectangular and there appear multiple jumps. The appearance of these jumps makes it necessary to define two field values with the help of which a hysteresis loop can be characterised. A value that marks the limit of metastability, called the *critical field*, and the other value which marks the magnetisation reversal, i.e. when the projection of the magnetisation on the field direction changes sign, and this is why it is called the *switching field* (or still coercive field).

B. Effect of the particle's size N

Here, we study the effect of varying the particle's size while keeping j and k_s fixed. So we use the same value of anisotropy constant for all spins and strong exchange, i.e. $k_s = 1, j = 10^2$, and vary the particle's diameter from 6 ($N = 56$) to 30 ($N = 12712$).

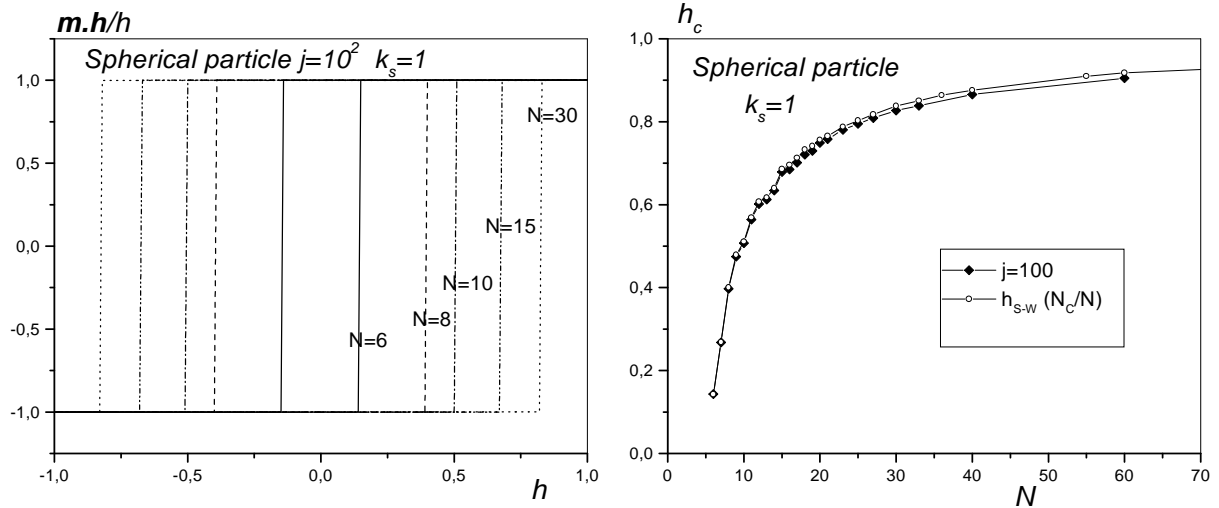


FIG. 8. Left: Hysteresis loops for $\psi = 0, k_s = 1, j = 10^2$ for different values of the particle's diameter N . Right: (in diamonds) Switching field for the same parameters as a function of the particle's diameter N . (in circles) SW switching field multiplied by the ratio of the number N_c of core spins to the total number of spins N .

In Fig. 8 (left) are presented hysteresis cycles of a particle with different when the field is along the core easy axis, and on the right the variation with the particle's diameter of the critical field [6] (in diamonds) obtained from the numerical solution of the Landau-Lifchitz equation for $j = 10^2$, and (in circles) the SW critical field multiplied by the core-to-volume ratio (see Eq. (8)). The figure on the left shows that for such a value of k_s the hysteresis loop is rectangular for all sizes, and that the critical field decreases with the particle's size. The latter fact is clearly illustrated by the figure on the right, which also shows that for $k_s = 1 = 10^{-2}j$, all these hysteresis loops can be scaled with those rendered by the SW model. Next, Fig. 9 shows the variation with the surface-to-volume ratio $N_{st} \equiv N_s/N$ of the critical field for all angles between the core easy axis and magnetic field, this is the limit-of-metastability curve. These results show that, even in the general case of a field applied at an arbitrary angle with respect to the core easy axis, the critical field of a spherical particle with $k_s = 1$ can be obtained from the SW model through a scaling with

constant N_c/\mathcal{N} . One should also note that the astroid for all particle sizes falls inside that of SW, in accordance with Fig. 8 (right), and the larger the surface contribution the more the astroid shrinks.

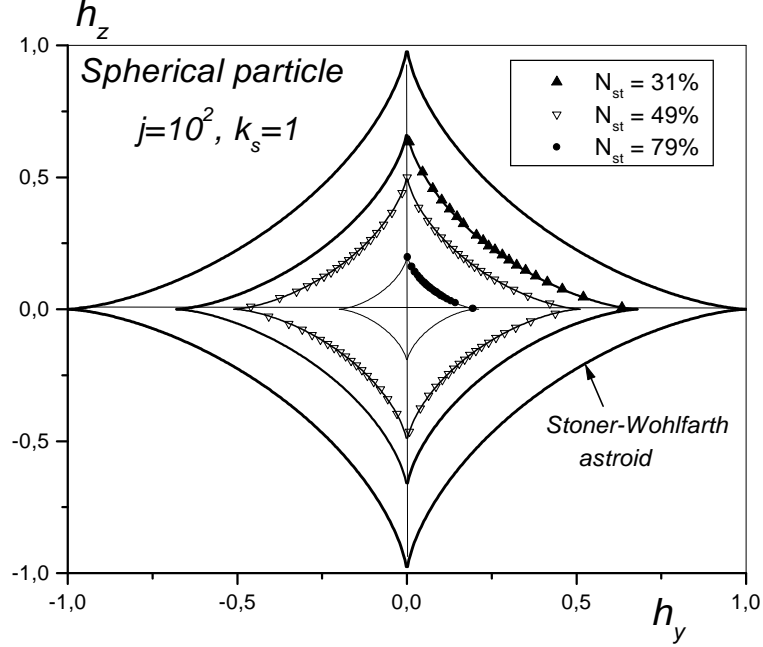


FIG. 9. Astroid for $k_s = 1, j = 10^2$ for different values of the surface-to-volume ratio $N_{st} \equiv N_s/\mathcal{N}$. The lines on the astroids inside the SW one are only guides for the numerical data.

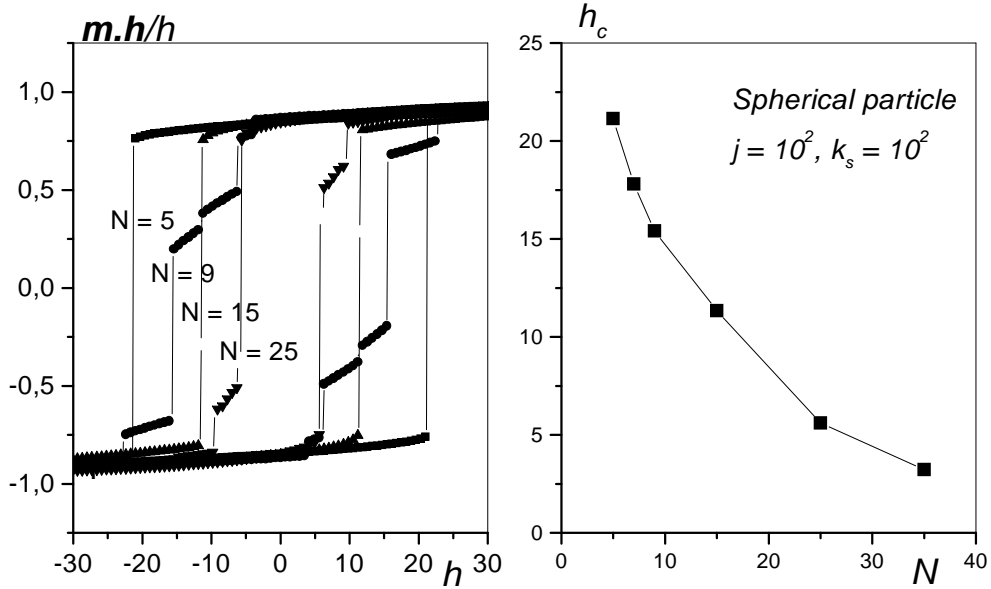


FIG. 10. Left: Hysteresis cycle for $\psi = 0, j = k_s = 10^2$, and different values of the particle's diameter N . Right: Switching field as a function of N for the same parameters.

Therefore, for $k_s = 1$ our results for the hysteresis loop and limit-of-metastability curve can be scaled with those of SW model with the scaling constant N_c/\mathcal{N} , which is smaller than 1 for a particle of any finite size.

Next, in Fig. 10 (left) we present the hysteresis loop in the case where the surface anisotropy constant k_s equals the exchange coupling and the field is applied along the core easy axis, and in Fig. 10 (right) the switching field [7] as a function of the particle's diameter N . There are two new features in comparison with the previous case of $k_s = 1$: the values of the switching field are much higher, and more importantly, its behaviour as a function of the particle's

size is opposite to that of the previous case. Indeed, here we see that this field increases when the particle's size is lowered. For such high values of k_s ($K_s \gg K_c$) surface spins are aligned along their easy axes, and because of strong exchange coupling they also drive core spins in their switching process. Thus, the smaller the particle the larger the surface contribution, and the larger the field required for complete reversal of the particle's magnetisation. This could explain the non-saturation of magnetisation that has been observed in e.g. cobalt particles [8].

C. Effect of the surface anisotropy constant k_s

Now, we fix the exchange coupling constant j , the particle's volume \mathcal{N} , and vary the surface anisotropy constant k_s . Because K_c is in general 2 to 3 orders of magnitude smaller than J , we have studied the effect of surface anisotropy constant in the case of $j = J/K_c = 10^2$.

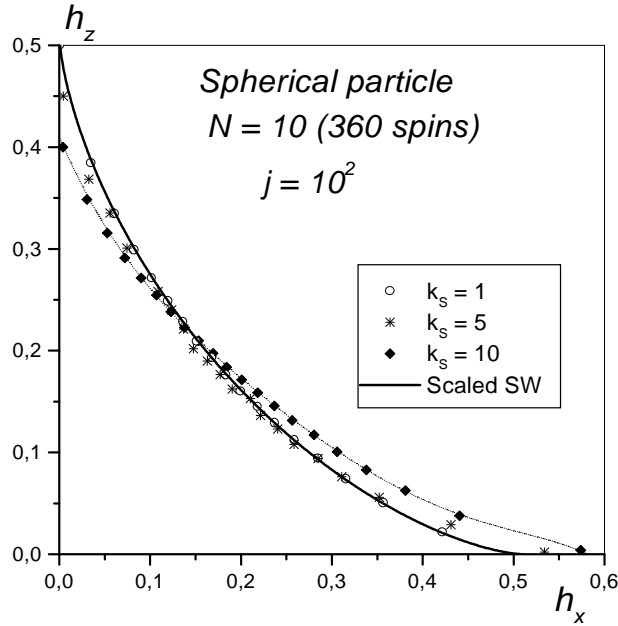


FIG. 11. Astroid for $j = 10^2$, $\mathcal{N} = 360$ and different values of surface anisotropy constant k_s . The full dark line is the SW astroid scaled with N_c/\mathcal{N} , but the dotted line is only a guide for the eye.

In contrast with the case $k_s = 1$ and $j = 10^2 - 10^3$ where the hysteresis loop and the limit-of-metastability curve scale with the SW ones with the same scaling constant for all angles between the applied field and core easy axis, we find that for $1 < k_s < 20$ the scaling constant depends on the angle ψ , as can be seen in Fig. 11. This fact explains the deformation of the SW astroid, that is a depression in the core easy direction and an enhancement in the perpendicular direction.

For larger values of k_s we have computed the hysteresis loop for $\psi = 0$, $\mathcal{N} = 360$, $j = 10^2$. The results are given in Fig. 12. Here, we first note that the shape of the hysteresis loop is rather different from that rendered by the SW model, since for $k_s = 30$, for instance, the hysteresis loop is no longer rectangular, even that $\psi = 0$. As explained earlier, this effect is due to the now more pronounced non-uniform rotation of surface spins and core spins located near the surface, and thereby that of the particle's magnetisation. This non-uniform switching process causes large deviations from the SW model, and thereby no simple scaling with the latter is possible.

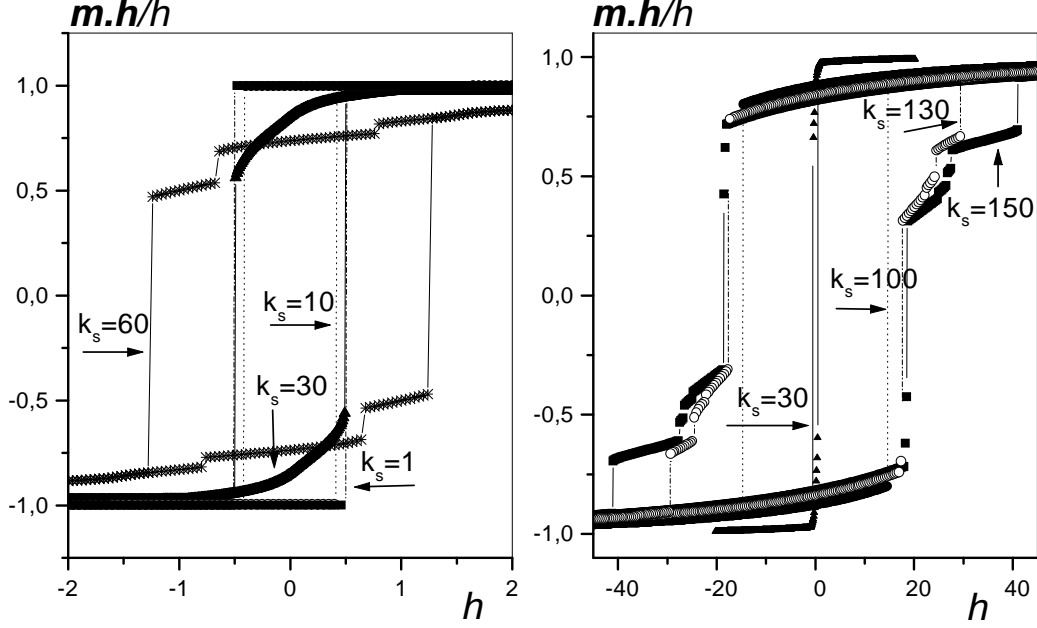


FIG. 12. Hysteresis loop for $\psi = 0$, $j = 10^2$, $N = 10$ and different values of surface anisotropy constant k_s . These two sets of data can not be presented as one plot because of scaling mismatch.

From Fig. 12, we extract and plot in Fig. 13 the switching field h_c as a function of k_s/j . We find that h_c first slightly decreases for $k_s/j \lesssim 0.1$ and then increases, and when k_s becomes of the order of j it jumps to large values. As discussed above, for such high values of k_s surface spins are aligned along their easy axes, and because of strong exchange coupling they also drive core spins in their switching process, which then requires a very strong field to be completed. Clearly, this particular value of the ratio k_s/j , i.e. $k_s/j = 1$, marks the passage from a regime where scaling with the SW results is possible (either with a ψ -dependent or independent constant) to the second regime where this scaling is no longer possible because of completely different switching processes.

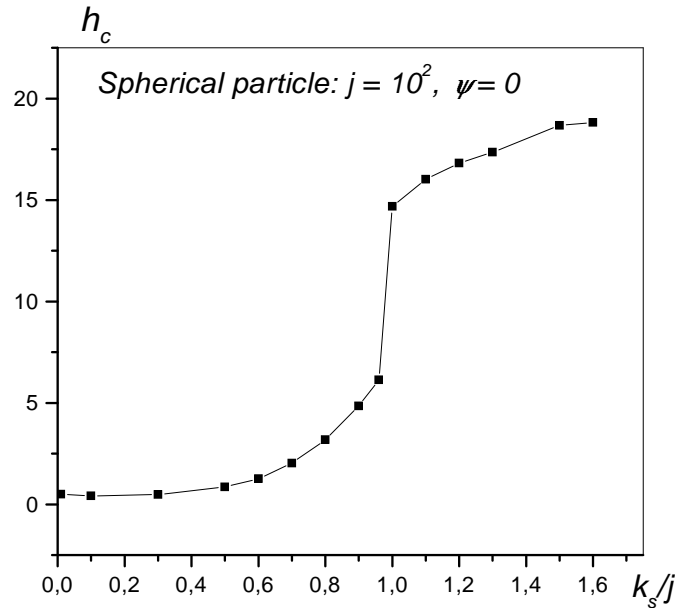


FIG. 13. Switching field versus the surface anisotropy constant for $\psi = 0$, $j = 10^2$, and $N = 10$.

Finally, when the field is applied at some non-zero angle with respect to the core easy axis, e.g. $\psi = \pi/4$, there

appear multiple large jumps at a smaller value of k_s (~ 20), i.e. even when this is of an order of magnitude smaller than j , see Fig. 14.

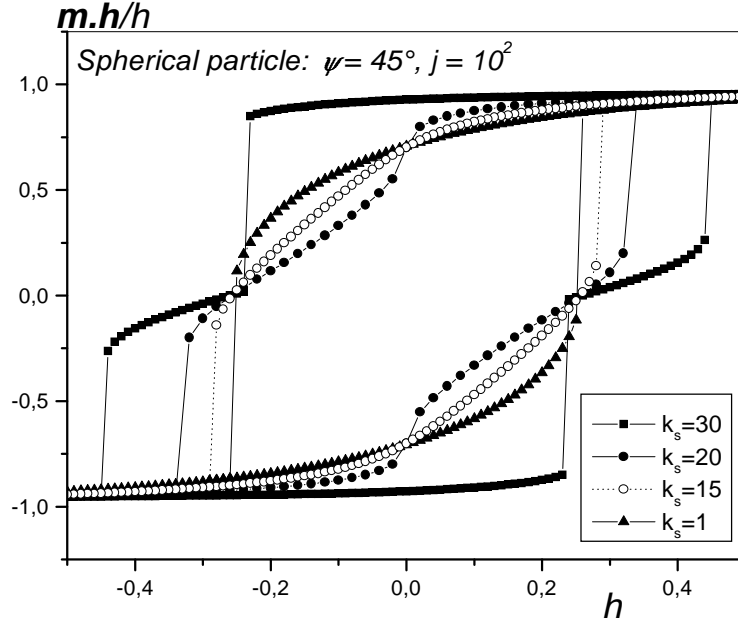


FIG. 14. Hysteresis for $\psi = 45^\circ$, $j = 10^2$, $N = 10$ ($\mathcal{N} = 360$) and different values of surface anisotropy constant k_s .

V. CONCLUSION

Our model of a spherical particle with uniaxial anisotropy in the core and radial anisotropy on the surface leads to mainly two pertinent regions for the surface anisotropy constant k_s , with $k_s > 1$, i.e. $K_s > K_c$:

- For small values of this parameter, e.g. $k_s/j \sim 0.01$ our model renders hysteresis loops and limit-of-metastability curves that scale with the SW results for all values of the angle ψ between the core easy axis and the applied field, the scaling constant being N_c/\mathcal{N} , which is smaller than 1 for a particle of any finite size. On the other hand, the critical field, which coincides in the present case with the switching field, increases with the particle's size and tends to the SW critical field in very large systems, and thereby the corresponding astroid falls inside the SW astroid for all particle sizes.

For larger values of k_s/j , but $k_s/j \lesssim 0.2$, we still have the same kind of scaling but the corresponding constant depends on ψ . This is reflected by a deformation of the limit-of-metastability curve. More precisely, the latter is depressed in the core easy direction and enhanced in the perpendicular direction. However, there is still only one jump in the hysteresis loop implying that the magnetisation reversal can be considered as uniform.

- For much larger values of k_s/j , starting from $k_s/j \simeq 1$, there appear multiple steps in the hysteresis loop which may be associated with the switching of spin clusters. The appearance of these steps makes the calculated hysteresis loops both qualitatively and quantitatively different from those of SW model, as the magnetisation reversal can no longer be considered as uniform, and one has then to define two characteristic values of the field associated with a hysteresis loop: the *critical field* and the *switching field*. In addition, in the present case, there are two more new features: the values of the switching field are much higher than in SW model, and more importantly, its behaviour as a function of the particle's size is opposite to that of the previous cases. More precisely, here we find that this field increases when the particle's size is lowered.

Consequently, considering the fact that experiments on nanoparticles show that the switching field does increase when the particle's size decreases (see e.g. [9] for cobalt particles), we may conclude that the anisotropy constant K_s is at least of the order of the exchange coupling J , inasmuch as we can assume radial anisotropy on the surface, as is usually done in the literature. Then, as discussed above, for such values of K_s , large deviations are observed with respect to the SW model in the hysteresis loop and thereby the limit-of-metastability curve, since in this case the

magnetisation reverses its direction in a non-uniform manner via a progressive switching of spin clusters. So to deal with these features one has to resort to microscopic approaches such as the one we used in this work.

Our model will be applied to cubo-octahedral cobalt particles with a diameter of ca. 3 nm recently studied in [10] (see also [11] for Pt particles). These are particles with fcc structure and truncated octahedrons on the surface, in which the core has a cubic anisotropy, and the surface anisotropy easy axes are believed to be along edges and facets with different constants K_s^α but whose values are uncertain at present. In our calculations we vary these parameters and study the effect of surface anisotropy on the Stoner-Wohlfarth astroid that has been experimentally measured in [10], where these anisotropy constants have been estimated from magnetic measurements. The final outcome of our calculations should give an estimation of K_s^α by comparing with these experimental results. This work is in progress.

ACKNOWLEDGEMENTS

We thank D.A. Garanin and M. Noguès for reading the manuscript and suggesting improvements.

* Electronic address (corresponding author HK): kachkach@physique.uvsq.fr

- [1] H. Kachkachi, A. Ezzir, M. Noguès, and E. Tronc, Eur. Phys. J. **B 14**, 681 (2000); H. Kachkachi and D.A. Garanin, *Boundary and finite-size effects in small magnetic systems*, to appear in Physica A, cond-mat/0001278.
- [2] E. C. Stoner and E. P. Wohlfarth, Philos. Trans. R. Soc. London, Ser. **A 240**, 599 (1948); IEEE Trans. Mag. MAG-27, 3475 (1991).
- [3] D.A. Dimitrov and G.M. Wysin, Phys. Rev. **B 50**, 3077 (1994).
- [4] H. Kachkachi and D.A. Garanin, Eur. Phys. J. **B22**, 291 (2001).
- [5] F.B. Hagedorn, J. Appl. Phys. **38**, 263 (1967); Al. Stancu, IEEE Trans. Mag. **33**, 2573 (1997).
- [6] For $k_s = 1$, there is only one jump in the hysteresis loop as can be seen in Fig. 8 (left). Hence, the critical field coincides with the switching field.
- [7] This is different from the critical field in the present case of $k_s = 10^2$.
- [8] M. Respaud, J. M. Broto, H. Rakoto, A. R. Fert, L. Thomas, B. Barbara, M. Verelst, E. Snoeck, P. Lecante, A. Mosset, J. Osuna, T. Ould Ely, C. Amiens, and B. Chaudret, Phys. Rev. B **57**, 2925 (1998).
- [9] J. P. Chen, C.M. Sorensen, K.J. Klabunde, and G.C. Hadjipanayis, Phys. Rev. **B 51**, 11527 (1995).
- [10] M. Jamet, W. Wernsdorfer, C. Thirion, D. Mailly, V. Dupuis, P. Mélinon, and A. Pérez, Phys. Rev. Lett **86**, 4676 (2001).
- [11] D.R. Rolison, in *Nanomaterials: Synthesis, Properties, and Applications*, edited by A.S. Edelstein and R.C. Cammarata, IOP 1998, p. 305.

